View metadata, citation and similar papers at core.ac.uk

brought to you by CORE

東北大学機関リポジトリ
TOUR
Tohoku University Repository

Micro-beam Analysis of Single Aerosol Particles at Tohoku University

著者	Matsuyama S., Ishii K., Yamazaki H., Kikuchi Y., Amartaivan Ts., Abe S., Inomata K., Watanabe Y., Ishizaki A., Oyama R., Kawamura Y., Suzuki A., Momose G., Yamaguchi T., Imaseki H.
journal or publication title	CYRIC annual report
volume	2006
page range	72-78
year	2006
URL	http://hdl.handle.net/10097/50364

V. 2. Micro-beam Analysis of Single Aerosol Particles at Tohoku University

Matsuyama S.[1], Ishii K.[1], Yamazaki H.[1], Kikuchi Y.[1], Amartaivan Ts.[1], Abe S.[1], Inomata K.[1], Watanabe Y.[1], Ishizaki A.[1], Oyama R.[1], Kawamura Y.[1], Suzuki A.[1], Momose G.[1], Yamaguchi T.[1], and Imaseki H.[2]

[1]Graduate School of Engineering, Tohoku University
[2]National Institute of Radiological Science

Introduction

Aerosol particles are caused by sandy dust, smoke from factories, exhaust gas of cars etc., and are thereafter often deformed by photo-chemical reactions in the atmosphere[1-3]. They are characterized by physical and chemical factors such as size, volume and chemical composition, and therefore carry information on the source of origin and the kind of generating process. Especially, elemental concentrations in atmospheric aerosol reflect the pollution sources and the processes generating air pollution. Therefore, elemental analysis of atmospheric aerosols is useful to search for the sources of aerosols. The combination of aerosol collection on thin filters and PIXE analysis is one of the most effective methods for analyzing atmospheric aerosols[1)] and many studies have focused on aerosol monitoring[1-5)]. These studies were carried out analyzing bulk samples thereby averaging over many single particles. In this case, statistical models, such as the principal components analysis (PCA) and the chemical mass balance (CMB), are needed to determine the contribution of different aerosol sources[5-8)]. Therefore, analysis of single aerosol particles is superior for obtaining information on source identification and for understanding the aerosol formation mechanism[6)]. In this study, we have developed a microbeam analysis system in order to analyze the elemental composition of single aerosol particles as well as their density with 1μm spatial resolution. Furthermore, by combining PIXE with RBS, off-axis STIM and STIM methods, we are capable of analyzing all elements and can determine the chemical composition of single aerosol particles.

Experiments

Aerosol samples were collected at the campus of Tohoku University for 3 days. The sampling position is located 10 m from a road traversing Aoba campus. Sampling times were ~6 hours in daytime and ~12 hours at night. In total 6 samples were collected. Aerosol particles were impacted on a thin polycarbonate film[7] at flow rates of 0.5*l*/min (face velocity: 265 cm/sec). The effective 50% cut-off diameter is estimated to be ~3 μm. Elemental concentrations and ratios in the polycarbonate film were obtained by fitting the RBS spectrum with the SIMNRA software[8]. Thickness of the film was estimated to be less than 0.3 μm, which is consistent with the one derived from the direct STIM measurements. The uniformity of the film is better than 10%. The thin polycarbonate film allows to measure protons scattered from the sample without spectral distortion by the film in RBS and off-axis STIM measurements as well as characteristic X-rays in PIXE.

Analysis was made using the microbeam analysis system at Tohoku University. Technical details of the microbeam and analysis system were presented in previous papers[9,10] and further development was carried out for the analysis of single aerosol particles. A schematic diagram of the improved setup is shown in Fig. 1. The system is composed of two X-ray Si(Li) detectors for PIXE analysis, an annular Si surface barrier detector for RBS analysis and a Si-PIN photodiode for direct and off-axis STIM analysis. Two X-ray detectors are set in vacuum at 115 degree with respect to the beam axis. The first one has large sensitive area (60 mm^2) and is suitable for trace elemental analysis. To reduce pile-up events or deformation of the spectrum by recoil protons, a Mylar filter (200 μm) was attached to the front of the detector. Maximum solid angle is ~0.13 sr. The second detector has a high-energy resolution (~136 eV), a thin Be entrance window (7.5 μm) and ~0.02 sr and is used to detect low energy X-rays. The system is capable of detecting X-rays ranging from 1 to 30 keV with good energy resolution and detection efficiency. The annular detector is very efficient, improving solid angle (~0.15 sr) without deteriorating angular spread and without interfering with the Si(Li) detectors. Mean scattering angle is 170 degree. A Silicon PIN-photodiode, a Faraday cup and a scintillator are attached to a detector wheel off center of the beam axis (see Fig. 1) for direct and off-axis STIM measurements. In direct STIM, the wheel is turned until the detector is centered on the beam axis. Scattering angle in off-axis STIM can be changed from 10 to 35 degree by rotating the wheel.

Analysis employed the following procedure. At first, direct STIM was carried out in a 500×500 μm^2 area defining the analysis area. After that, simultaneous

PIXE/RBS/off-axis STIM measurements used a scanning area of 40×40 μm^2 to 100×100μm^2. Energy of the proton beam is 3 MeV and beam spot size is 1×1 μm^2 with a beam current of 50~100 pA. Total accumulated charge was 0.1~0.5 μC. After the measurement, direct STIM is employed once more for the same position to check for deformation of the sample. Two or three positions were analyzed for 1 sample.

Quantitative PIXE analysis was performed using the GeoPIXEII software[11]. After generating the elemental maps, particles to be analyzed were selected from these maps and PIXE, RBS and off-axis STIM spectra were extracted. Elemental composition for elements heavier than Na was deduced from fitting of the extracted PIXE spectra of single aerosol particles. In total 270 particles were analyzed and Na, Mg, Al, Si, P, S, Cl, Ca, Ti, Mo, Fe, Ni, Cu, Zn and Br elements were quantified.

Quantitative analysis of hydrogen was carried out by analyzing the extracted off-axis STIM spectra. Figure 2 shows typical off-axis STIM spectra from an aerosol particle compared with spectra from the backing film. The intensity of protons scattered from the backing is very low compared to scattering from aerosol particles and is thus easily subtracted. The scattering angle was set to 28 degrees, which suffices to separate proton peaks scattered from heavy elements and from hydrogen even in a thickness of 50 μm of organic film. While intensity of scattered protons decreases with increasing scattering angle, the counting rate of hydrogen at 28 degrees is sufficient for analysis. For the quantitative analysis of hydrogen, intensities of hydrogen were calibrated by measuring hydrogen yields from polycarbonate films of different thickness. The relation between hydrogen peak yield and hydrogen quantity is linear and is used to calibrate the quantitative analysis of hydrogen.

Light elements (C,N,O) were quantified by analyzing the extracted RBS spectra. Figure 3 shows RBS spectra for an aerosol particle compared with spectra from the backing. For the analysis of single aerosol particles, a similar analysis by using SIMNRA software might be efficient for quantitative analysis. However, samples might not be uniform even in a single aerosol and experimental scattering cross sections are scarce for major elements of aerosols. Therefore, concentration of carbon and oxygen were derived from peak yields which were calibrated by measuring peak yields from polycarbonate films of known thickness. Since scattering cross section of C(p,p)C and O(p,p)O for 3 MeV to 2.8 MeV are constant within 5%[12], this method is effective for quantitative analysis if peaks from the

sample are well separated and nitrogen is thus not included in yields. Since carbon peak and oxygen peak in the RBS spectra overlap when energy loss is larger than 100 keV, particles whose energy losses were larger than 100 keV were excluded. Even if energy loss was below 100 keV, spectra with overlapping peaks were excluded as nitrogen may be included. In the present analysis, 70 particles were excluded.

Results

Figure 4 shows typical elemental and direct STIM maps with a micrograph and scale. The direct STIM map shows the density distribution corresponding to the micrograph. Direct STIM is then used to define the position of analysis. Elemental loss was not observed. The elemental distribution of Al equals to the one of Si, originating mainly from soil dust of Alumino-Silicate particles. Ca and S elements also show similar distributions and may originate from $CaSO_4$ particles. Na, Mg and Cl elements come from marine aerosols, and shows similar distributions. The light elements, hydrogen and carbon show similar distribution, and all these particles are clustered into Si-rich, Ca-rich and Fe-rich and marine aerosols groups, according to their major elements. The soil and marine aerosols are 60% and 20% of total particles, respectively.

Correlation functions between Ca and S and between Ca and O are shown in Figs. 5 and 6. As Ca increases, both S and O increase. Especially, particles whose sum of Ca and S mass is higher than 50% of the total mass are well correlated. Correlation between Ca and H also shows similar trend. Ca, S, O and H are well correlated and atomic ratio of Ca:S:O:H is 1:0.7:12:12 for these particles. These particles appear to contain $CaSO_4$ particles. Since $CaSO_4$ is stable in the presence of H_2O, the ratio of O to Ca is higher than 4, because H_2O is also present in $CaSO_4(H_2O)_n$.

Figure 6 shows correlation between H and C. C increases as H increases and the atomic ratio is around 1. Figure 7 shows atomic percentage of H and C. Total mass of aerosol particles was derived from the sum of H, C and O mass after background subtraction of polycarbonate backing. Data are distributed around the line which shows atomic ratio of 1. Atomic ratio of oxygen is 0.1 to 0.5. It may imply that organic material is based on aromatic series mixed with -COOH radical.

Conclusions

We have developed a microbeam analysis system in order to analyze single aerosol particles with 1μm spatial resolution. By combining PIXE with RBS, off-axis STIM and

direct STIM methods and by using thin backing film, we can quantify single aerosol particles containing elements from hydrogen to heavy metals, thus revealing the chemical composition of these particles. The chemical composition provides information on source identification and leads to better understanding of the aerosol formation mechanism. The described micro-beam analysis system represents a powerful research tool for aerosol particles, emission source identification and for a better understanding of the aerosol formation processes.

Acknowledgements

This study was partly supported by Grant-in-Aid for Scientific Research (S) No. 13852017 and Grant-in-Aid for Scientific Research in Priority Areas under Grant No.14048213 from the Ministry of Education, Culture, Sports, Science and Technology, Japan. The authors would like to thank Mr. K.Komatsu, T.Nagaya and C.Akama for their help in constructing the microbeam and target system.

References

1) Ariola V. et. al., *Nucl. Instr. and Meth*., **B190** (2002) 471.
2) Parti P. et. al., *Atmospheric Environment*, **34**, 3 (2000) 149.
3) Bongiovanni S.F. et. al., *Nucl. Instr. and Meth*., **B161-163** (2000) 786.
4) Cohen D.D, *Nucl. Instr. and Meth*., **B136-138** (1998) 14.
5) Formenti P., Annegarnand H.J., Piketh S.J., *Nucl. Instr. and Meth.*, **B136-138** (1998) 948.
6) Orlic I., Osipowicz T., Watt F., Tang S.M., *Nucl. Instr. and Meth*., **B104** (1995) 630.
7) Yamazaki H., Tsutsumi K., Ishii K., Matsuyama S., Murozono K., Inoue J., Iwasaki S., *Int. J. of PIXE*, **7**(1&2) (1997) 101.
8) Mayer M., SIMNRA Users's Guide, Technical Report IPP 9/113, MPI Plasmaphysik, Garching, Germany, 1997.
9) Matsuyama S., Ishii K., Yamazaki H., Sakamoto R., Fujisawa M., Amartaivan Ts., Ohishi Y., Rodriguez M., Suzuki A., Kamiya, T. Oikawa M., Arakawa K., Matsumoto N., *Nucl. Instr. and Meth.* , **B210** (2003) 59.
10) Matsuyama S., Ishii K., Yamazaki H., Barbotteau, Y. Amartivan Ts., Izukawa D., Hotta K., Mizuma K., Abe, S. Oishi Y., Rodriguez M., Suzuki A., Sakamoto R., Fujisawa M., Kamiya T., Oikawa M., Arakawa K., Imaseki H., Matsumoto N., *Int. J. of PIXE*, **14** (1&2) (2004) 1.
11) Ryan C.G., Van Achterbergh E., Yeats C.J., Drieberg S.L., Mark, G. McInnes B.M., Win T.T., Cripps G., Suter, G.F., *Nucl. Instr. and Meth.*, **B188** (2002) 18.
12) Amirikas R., Jamieson D.N., Dooley S.P., *Nucl. Instr. and Meth.*, **B77** (1993) 110.

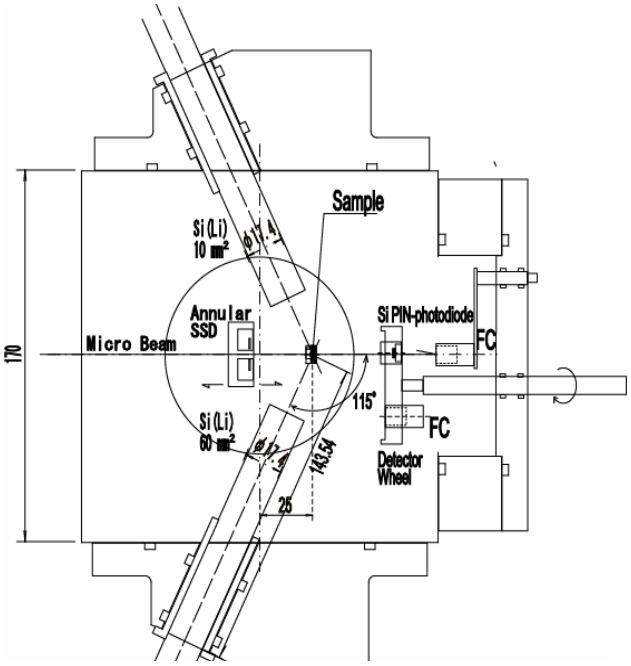

Figure 1. Schematic diagram of the analysis system.

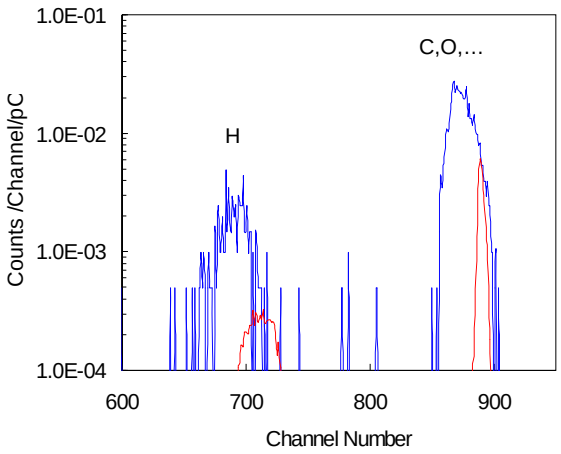

Figure 2. Typical off-axis STIM spectra from an aerosol particle (-) and from a backing film (-).

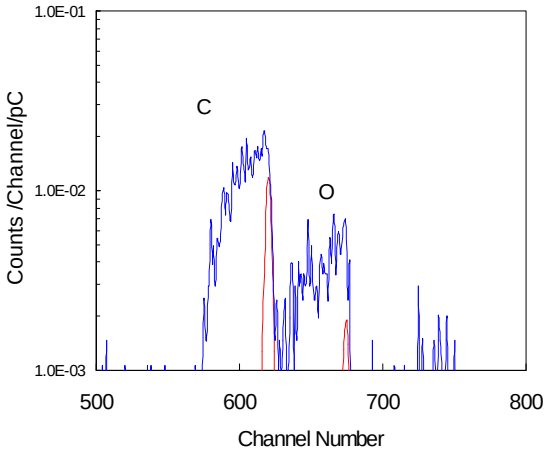

Figure 3. RBS spectra from a aerosol particle (-) and from a backing film (-).

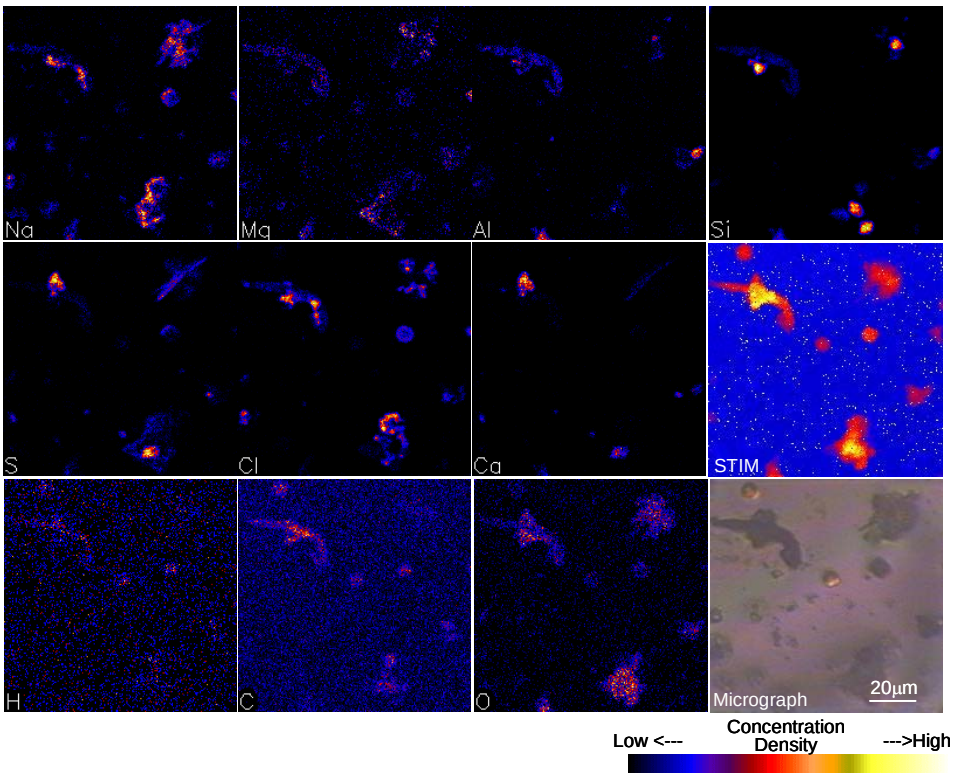

Figure 4. Typical elemental maps with a micrograph.

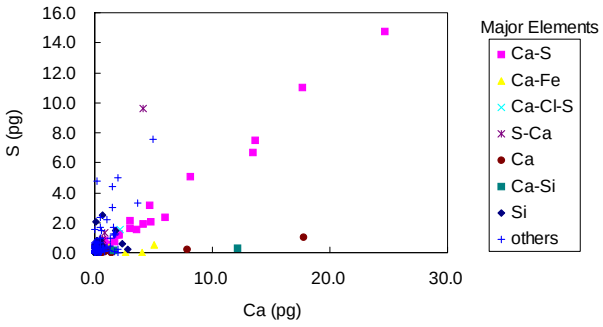

Figure 5. Correlation between Ca and S.

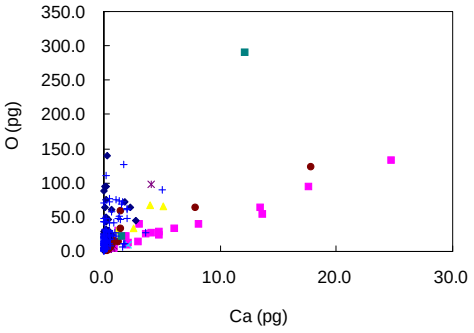

Figure 6. Correlation between Ca and O.

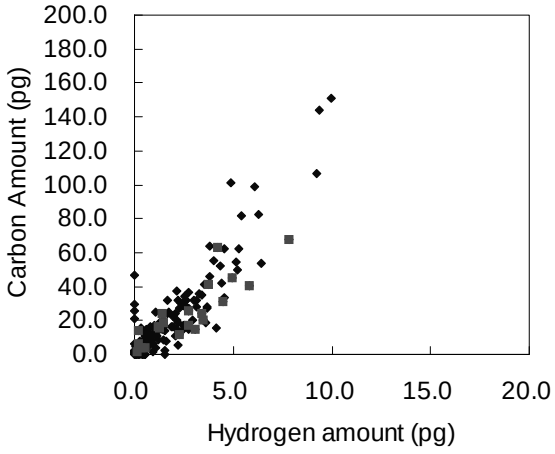

Figure 7. Correlation between H and C.

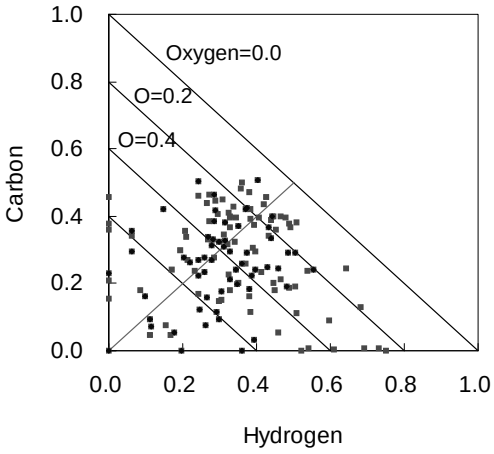

Figure 8. Atomic percentage of H and C.